Contribution of Sea Ice Loss to Arctic Amplification

Arun Kumar[1], Judith Perlwitz[2], Jon Eischeid[2], Xiaowei Quan[2], Taiyi Xu[2], Tao Zhang[2], Martin Hoerling[2], Bhaskar Jha[1], and Wanqui Wang[1]

[1] *NOAA/NCEP, 5200 Auth Road, Camp Spring MD20746, USA*
[2] *NOAA/ESRL, 325 Broadway, Boulder, CO80305, USA*

ABSTRACT

Atmospheric climate models are subjected to the observed sea ice conditions during 2007 to estimate the regionality, seasonality, and vertical pattern of temperature responses to recent Arctic sea ice loss. It is shown that anomalous sea ice conditions accounted for virtually all of the estimated Arctic amplification in *surface-based* warming over the Arctic Ocean, and furthermore they accounted for a large fraction of Arctic amplification occurring over the high-latitude land between 60°N and the Arctic Ocean. Sea ice loss did not appreciably contribute to observed 2007 land temperature warmth equatorward of 60°N. Likewise, the observed warming of the *free atmosphere* attributable to sea ice loss is confined to Arctic latitudes, and is vertically confined to the lowest 1000 m. The results further highlight a strong seasonality of the temperature response to the 2007 sea ice loss. A weak signal of Arctic amplification in surface based warming is found during boreal summer, whereas a dramatically stronger signal is shown to develop during early autumn that persisted through December even as sea ice coverage approached its climatological values in response to the polar night.

1. Introduction

The 2007 annual temperatures averaged over land areas poleward of 60°N were the warmest in the instrumental record since 1875 (Bekryaev et al. 2010). The retreat of Arctic sea ice was also unprecedented, with the September 2007 annual minimum sea ice extent eclipsing

the previous observational record low (Stroeve et al. 2008). Such extreme climate-cryospheric conditions were not isolated episodes, in so far as they link to trends of accelerating warming over the northern polar land area (e.g., Lawrence et al. 2008; Bekryaev et al. 2010) and to accelerating sea ice loss during the last decade (e.g. Stroeve et al. 2007; Deser and Tang 2008).

The debate on whether and when Arctic amplification of near-surface air temperature rise would emerge was posed as an open question based on temperature data through the end of the 20th Century (Serreze and Francis 2006). The subsequent decade of observational (Bekryaev et al. 2010) and model based reanalysis products (Screen and Simmonds 2010) in the new millennium has confirmed the existence of a strong Arctic amplification. Annual land temperatures poleward of 60°N during 1979-2008 have risen at twice the rate of the Northern Hemisphere value (Bekryaev et al. 2010), and the surface amplification of warming trends is seen in all seasons except boreal summer (Screen and Simmonds 2010).

This study estimates the impact of observed Arctic sea ice loss on recent climate condition by identifying the sensitivity of surface and free atmospheric temperatures to the sea ice anomalies of 2007. In addressing recent, actual conditions, this study is distinct from Deser et al. (2010) who examined sea ice impacts on potential conditions at the end of the 21st century. The approach involves atmospheric general circulation models (AGCMs) subjected to the observed monthly variations of sea ice and sea surface temperature (SST) conditions, methods similar to those employed in previous studies of sea ice impacts on climate (e.g., Alexander et al. 2004; Deser et al. 2004).

2. Data and model simulations

a. Observations

To obtain the best estimate of the near-surface temperature change north of 50°N , we blend three observational data sets without obvious discontinuities: the U.K. Hadley Center's HadCRUT3v (Brohan et al. 2006), the National Oceanic and Atmospheric Administration (NOAA) Land/Sea Merged Temperatures (Smith and Reynolds 2005), and the NCEP/NCAR-R1 reanalysis (Kalnay et al. 1996). All data are spatially interpolated to a common T63 model grid. The data are merged as follows: the NOAA and CRU temperature fields are averaged for land regions 50°N-60°N; the NOAA, CRU and reanalysis data are averaged between 60°N-70°N. Temperatures north of 70^{o}N, which mainly consists of the Arctic Ocean domain, are based on reanalysis. We also present latitude-height sections of air temperatures that are based on NCEP/NCAR-R1 reanalysis. The reference period for anomalies is 1971-2000. Serreze et al (2009) noticed several shortcomings and errors of the NCEP/NCAR-R1 related to sea ice treatment. Therefore, our analysis over land area relies as much as possible on observations and not on the NCEP/NCAR-R1.

b. Models

We utilize three atmospheric general circulation models: NCAR Community Climate Model: CCM3 (Kiehl et al. 1996); Geophysical Fluid Dynamics Laboratory Atmospheric Model Version 2.1 (GFDL AM2.1) (Delworth et al. 2006) and a version of the National Centers for Environment Prediction (NCEP) Global Forecast System (GFS) used as atmospheric model component in the NCEP Climate Forecast System (Saha et al. 2006 The lower boundary SST and sea ice is based on the merged Hadley-OIv2 SST and sea ice concentration. This new SST dataset SST takes into account regional details for ice coverage and no longer sets SST to -1.8C when ice concentration exceeds 90% (see Hurrell et al. 2008 for details on the merging procedure). Use of these boundary conditions in model simulations rectifies errors in sea ice

extent noted by Serreze et al (2009) for the NCEP/NCAR-R1.

Twin parallel 50-member ensemble simulations are performed for each of the AGCMs. In one set, the so-called control experiments, the monthly 2007 SSTs are specified whereas the sea ice conditions are specified to be the 1971-2000 climatological seasonal cycle. In the second set, the so-called sea ice forced experiments, we again specify the 2007 SST conditions but use the observed 2007 monthly evolving sea ice conditions. The sea ice response is inferred as the difference between the ensemble mean of the AGCM simulations forced with the observed 2007 SST and sea ice and the ensemble mean of control experiments. Each realization is begun from arbitrary atmospheric initial conditions in October, and extends for a 15-month period through December 2007. We will discuss only the multi-model response based on the three AGCMs. We note however that the response is very robust among the individual models. In our analysis we do not estimate the sensitivity to changes in sea ice thickness (or to other changes in sea ice properties, e.g., optical properties, surface roughness etc.) which may also affect the response to some extent (Deser et al. 2010).

3. Results

The climatological seasonal cycle of Arctic sea ice area is characterized by a September minimum and a March maximum (Fig. 1, left, blue curve). In 2007, however, the seasonal cycle exhibited far greater amplitude than normal due to a precipitous decline in the September minimum (Fig, 1, left, red curve). According to the analysis of Stroeve et al. (2008), the extent of sea ice in September 2007 was 50% less than in the 1950s to 1970s prior to the onset of a long-term decline in September Arctic sea ice.

The spatial pattern of sea ice conditions for both June-August (Fig. 1, middle) and September-November 2007 (Fig. 1, right) reveals that most of the sea ice loss occurred along the

northern Siberian and Alaskan coast (Fig. 1, right). The loss accelerated with the seasonal cycle. Indeed, at the time of its minimum in September 2007, the Northwest Passage from Baffin Bay towards M'Clure Strait, connecting Atlantic to the Pacific, was open.

Figure 2 shows the spatial patterns of observed 2007 summer (top) and autumn (bottom) surface temperature anomalies poleward of 50°N. A strong Arctic amplification of surface-based warming is evident by autumn. Further analysis of monthly evolving surface temperatures over the Arctic Ocean region (not shown) reveals an abrupt emergence of warm conditions in September in concert with the month of largest sea ice loss. And, whereas Arctic Ocean sea ice extent grew in subsequent months in response to the polar night--- causing sea ice conditions to approach near-normal values, very warm surface air temperature over the Arctic Ocean nonetheless persisted through December 2007.

It is evident that the much larger air-sea temperature contrasts during polar night provide for a enhanced surface-based heat source that compensates for the gradual reduction of open Arctic Ocean waters by late autumn so as to continue to warm Arctic temperatures (see also Lu and Cai 2009; Deser et al. 2010). Consistent with this notion of strong heat exchange between the ocean and atmosphere, vertical cross sections of the 2007 temperature anomalies exhibit a distinct lower troposphere warming, with an Arctic maximum in autumn, though no such signature in summer (Fig. 2, right panels). A similar seasonality and vertical structure of Arctic amplification is described by Screen and Simmonds (2010) who analyzed observed Arctic temperature trends for 1989-2008. It is also a distinctive feature of model simulated responses when forced by projected Arctic sea ice loss in the late 21st Century due to anthropogenic forcing (Deser et al. 2010).

We next estimate the influence of Arctic sea ice anomalies on temperature from the sea ice forced AGCM simulations. The AGCM simulated temperature responses are shown in Fig. 3. The seasonal contrast in the amplitude and the spatial pattern of the surface temperature response during summer (July-August) versus autumn (September-November) is similar to that seen in observations--the models simulate a much weaker amplitude in the summer temperature response to sea ice loss (Fig. 3, top) compared to their autumn counterpart (Fig. 3, bottom). Likewise, the models also generate strong warm anomalies over the Arctic through December 2007 that is analogous to the observed conditions (not shown). In both seasons one can discern a distinct latitudinal asymmetry to surface warming, and is likely dictated by the pattern of sea ice loss. Not surprisingly, the largest warming is concentrated over the oceanic regions of greatest sea ice decline. And, owing to the fact that sea ice decline was most extensive along the Siberian and Alaskan sectors of the Arctic Ocean, the strongest land temperature warming occurs over northern Siberia and northern Alaska and the Canadian Northwest Territory. These spatial features are also evident in the observed pattern of temperature anomalies, although warming extends into lower polar latitudes in observations than in the model simulations. The vertical structure of the AGCM simulated zonal mean temperature response during summer (Fig. 3, top right) and autumn (Fig. 3, bottom right) reveals that the sea ice loss impact is confined to the lowest 1000 meters above the surface. This is to be contrasted with the observed warming pattern that stretched throughout much of the troposphere (see Fig. 2), suggesting that processes other than sea ice loss were mostly responsible for warming above 1000m.

The observed 2007 temperature anomaly could result from multiple factors including sea ice impacts, other boundary effects such as global SST and other land surface conditions, the direct radiative effect of anthropogenic greenhouse gases (GHGs) and aerosols, and also from

purely internal atmospheric variability. By contrast, the ensemble mean AGCM simulated anomaly in our experiments isolates the response to 2007 sea ice conditions only. Regarding the simulated latitudinal pattern of the warming, it is clear that a autumn season Arctic amplification signal of sea ice loss in the low troposphere explains most of the observed Arctic amplification, and that other processes were of secondary importance The abrupt poleward increase in surface and low tropospheric warmth occurring in observations and ensemble model responses indicates that the recent Arctic amplification is very likely the result of sea ice loss.

The large ensemble of experiments conducted for 2007 facilitates an estimate of internal atmospheric variability, thereby addressing the question whether the recent Arctic amplification could be reconciled with random atmospheric processes. Figure 4 presents the full probability distribution function (PDF) of seasonal temperatures that are constructed from the individual 150-member realizations. Since each ensemble member was subjected to identical boundary forcings, the spread of the PDFs is an indication of efficacy of internally generated atmospheric variability, and the ratio of the ensemble mean anomaly (i.e., PDF mean shift) to the noise (i.e., PDF spread) estimates the signal-to-noise ratio. Table 1 summarizes these statistical properties for summer and autumn, and the plotted numbers in Fig. 4 (inset) are the signal-to-noise ratios for various sub-regions including all Arctic Ocean points poleward of 65°N (red curve), all land points between 50^{o}-60^{o}N (black curve), and Arctic high-latitude land (all land points between 60°N to 90°N. (orange curve). For comparison, area-averaged observed surface temperature anomalies are also shown as dots above each PDF.

Figure 4 clearly indicates that anomalous sea ice conditions accounted for virtually all of the observed Arctic amplification in surface-based warmth over the Arctic Ocean. The signal-to-noise ratio of 3.8 in summer and 6.6 in winter indicates the high detectability of this warming

signal, and indicates that the observed autumn 2007 warming over the Arctic Ocean of about +4°C was very unlikely due to atmospheric noise. Over the high-latitude land region (north of 60°N) during autumn, the signal of warming induced remotely by the Arctic sea ice loss is nearly twice the standard deviation of temperature fluctuations that could arise from atmospheric variability only, suggesting that the observed high-latitude land warming of about +2°C was strongly influenced by the remote sea ice conditions. By contrast, the observed warming in sub-Arctic land regions between 50°-60°N of about +1°C in both summer and autumn are inconsistent with a remote impact of Arctic sea ice loss alone, although it is within the envelope of realizable outcomes associated with atmospheric variability.

4. Concluding Remarks

Our study is the first attempt to estimate the strength, spatial structure and seasonality of observed sea ice loss on recent climate conditions. In using a modeling approach, this study clarifies the interpretation of the sea ice role in observed Arctic amplification. This could be previous only be speculated upon from the various empirical studies. We found that an extreme Arctic sea ice loss in 2007 has a spatially confined temperature response which is limited to the region north of 60^{o}N and to the lowermost atmosphere, and which is most pronounced during autumn and early winter. The spatial structure of Arctic amplification due to sea ice loss is strongly determined by the specific spatial structure of sea ice loss pattern itself.

The observed 2007 sea ice loss is part of a longer-term downward trend. Furthermore, the observed changes in Arctic sea ice extent and thickness are consistent with an increase in anthropogenic GHGs and aerosols, although observed changes are occurring faster that predicted by climate models (Serreze et al. 2007). The study by Wang and Overland (2009) reveals that the Arctic sea ice anomaly pattern which is projected to occur in response to increased GHG

concentrations over the next several decades is similar to the observed anomaly structure in 2007. The implication is that the spatial pattern of surface temperature response to recent Arctic sea ice loss may be symptomatic of the response patterns anticipated from anthropogenic forcing. Nonetheless, given that sea ice conditions are also sensitive to the influence of natural fluctuations (for instance, ocean heat transports, the variability in the Beaufort gyre etc.) an open question is how the spatial pattern of high latitude temperature anomalies would change if the pattern of sea ice loss itself changed.

The results reveal that consideration of sea ice loss is an important factor in the attribution of recent climate variability and trends in the Arctic region, and are consistent with the emerging view of the role of the sea ice on the high latitude atmospheric circulation variability (Francis et al. 2009). Our study focused solely on the direct impact of sea ice loss on the magnitude of Arctic warming and its spatial extent, and confirms that it is the principal factor responsible for Arctic amplification of warming trends. Our study does not address the role of other changes in the climate system that are evolving in response to increased greenhouse gases including changes due to the direct radiative impact of the GHG forcing, and associated GHG-forced changes in sea surface temperature and atmospheric circulation that can affect high latitude temperatures. It is evident from the critical role of sea ice that initialization of sea ice conditions will be central toward advancing improved predictions of annual to decadal climate conditions in the Arctic.

References

Alexander, M.A., and Co-authors, 2004: The atmospheric response to realistic Arctic sea ice anomalies in an AGCM during winter. *J.Climate,* **17**, 890–905.

Bekryaev, R. V., I. V. Polyakov, V. A. Alexeev, 2010: Role of polar amplification in long-term surface air temperature variations and modern arctic warming. *J. Climate*, in print, doi: 10.1175/2010JCLI3297.1

Brohan, P., J. J. Kennedy, I. Harris, S. F. B. Tett, and P. D. Jones, 2006: Uncertainty estimates in regional and global observed temperature changes: A new dataset from 1850, *J. Geophys. Res.*, **111**, D12106, doi:10.1029/2005JD006548.

Delworth, T. L. and Co-authors, 2006: GFDL's CM2 Global Coupled Climate Models. Part I: Formulation and simulation characteristics. *J. Climate*, **19**, 643-674.

Deser, C., G. Magnusdottir, R. Saravanan, and A. S. Phillips, 2004: The effects of North Atlantic SST and sea ice anomalies on the winter circulation in CCM3. Part II: Direct and indirect components of the response. *J. Climate*, 17, 877–889.

Deser, C., and H. Teng, 2008: Recent trends in Arctic sea ice and the evolving role of atmospheric circulation forcing, 1979–2007. Arctic Sea Ice Decline: Observations, Projections, Mechanisms, and Implications, Geophys. Monogr., Vol. 180, Amer. Geophys. Union, 7–26.

Deser, C., R. Tomas, M. Alexander, D. Lawrence, 2010: The seasonal atmospheric response to projected arctic sea ice loss in the later twenty-first century. *J. Climate*, **23**, DOI: 10.1175/2009JCLI3053.1

Francis, J. A., and Co-authors, 2009: Winter northern hemisphere weather patterns remember summer arctic sea-ice extent. *Geophys. Res. Lett*, **36,** L07503, doi:10.1029/2009GL037274.

Hurrell, J.W., J.J. Hack, D. Shea, J.M. Caron, and J. Rosinski, 2008: A new sea surface temperature and sea ice boundary data set for the Community Atmosphere Model,

Journal of Climate, Vol. 21, 5145-5153.

Kalnay, E. and Coauthors, 1996: The NCEP/NCAR 40-year Reanalysis Project. *Bull. Amer. Meteor. Soc.*, **77**, 437-471.

Kiehl, J., and Co-authors, 1998: The National Center for Atmospheric Research Community Climate Model: CCM3. *J. Climate*, **11**, 1131-1149.

Lawrence, D. M., A. G. Slater, R. A. Tomas, M. M. Holland, and C. Deser, 2008: Accelerated Arctic land warming and permafrost degradation during rapid sea ice loss. *Geophys. Res. Lett.*, **35**, L11506, doi:10.1029/2008GL033985.

Lu, J.-H., and M. Cai, 2009: Seasonality of polar surface warming amplification in climate simulations. *Geohpys. Rev. Lett.*, **33**, doi:10.1029/2009GL040133.

Saha, S., and Coauthors, 2006:, The NCEP Climate Forecast System. *J. Climate*, **19**, 3483-3517.

Serreze, M. C., and Francis, J. A., 2006: The Arctic amplification debate. *Climatic Change*, **76**, 241–264.

Serreze, M. C., M. M. Holland, and J. Stroeve. 2007. Perspectives on the Arctic's shrinking sea ice cover. *Science* 315(5818): 1533-1536, doi:10.1126/science.1139426.

Serreze, M. C., A. P. Barrett, J. C. Stroeve, D. N. Kindig, and M. M. Holland. 2009. The emergemce of surface-based Arctic. *The Cryosphere* 3: 11–19.

Screen, J. A., and I. Simmonds, 2010: The central role of diminishing sea ice in recent arctic temperature amplification. *Nature*, **464**, doi:10.1038/nature09051.

Smith, T. M., and R. W. Reynolds, 2005: A global merged land air and sea surface temperature reconstruction based on historical observations (1880–1997), *J. Climate*, **18**, 2021–2036, doi:10.1175/JCLI3362.1.

Stroeve, J., M. M., Holland, W. Meier, T. Scambos, and M. Serreze, 2007: Arctic sea ice decline: faster than forecast. Geophys. Res. Lett. 24, L09501, doi:10.1029/2007GL029703.

Stroeve, J. M., and co-authors 2008. Arctic sea ice plummets in 2007. *Eos, Trans. Am. Geophys. Un*. **89**, 13–20.

Wang, M., and J. E. Overland, 2009: A sea ice free summer Arctic within 30 years? *J. Geophys. Res.*, **36**, L07502, doi:10.1029/2009GL037820.

Figure Caption

Figure 1: Arctic sea ice area determined based on area of ocean with at least 50% sea ice concentration. *Left*: seasonal cycle (blue: 1971-2000 climatology, red: 2007). *Center and right:* Maps of Jun.-Aug. and Sep.-Nov. average respectively (blue contour: 1971-2000 climatology, shaded in red: 2007 anomaly).

Figure 2: Maps of observed near surface temperature anomalies (left) and latitude-height sections of zonal mean air temperature anomalies based on the NCEP/NCAR-R1 reanalysis (right) for 2007 Jun.-Aug. average (top) and 2007 Sep.-Nov. average (bottom). The year 2007 anomalies are calculated relative to the base period 1971 to 2000.

Figure 3: Same as in Fig. 2 but for simulated temperature response.

Figure 4: Probability Distribution Functions of simulated near surface temperature response averaged (i.e., area-weighted over grid points) over Arctic Ocean north of 60^{o}N (red), over land north of 60^{o}N (orange), and land area between 50 and 60^{o}N (black). *Left*: Jun.-Aug. 2007. *Right:* Sep.-Nov. 2007. Numbers in the legend indicate signal to noise ration of the response. The dots in similar colors indicate anomalies from the blended surface temperature data set averaged over the grid points for the different regions.

Table 1: Mean and standard deviation of area averaged near surface air temperature responses (°C) to 2007 Arctic sea ice loss based on 150 ensemble members for summer (June-August) and autumn (September-November)

Season	Arctic Ocean	High-latitude land (>60°N)	Land 50°N-60°N
Summer	0.8 ± 0.21	0.4 ± 0.50	0.05 ± 0.60
Autumn	4.1 ± 0.62	1.3 ± 0.77	0.2 ± 0.91

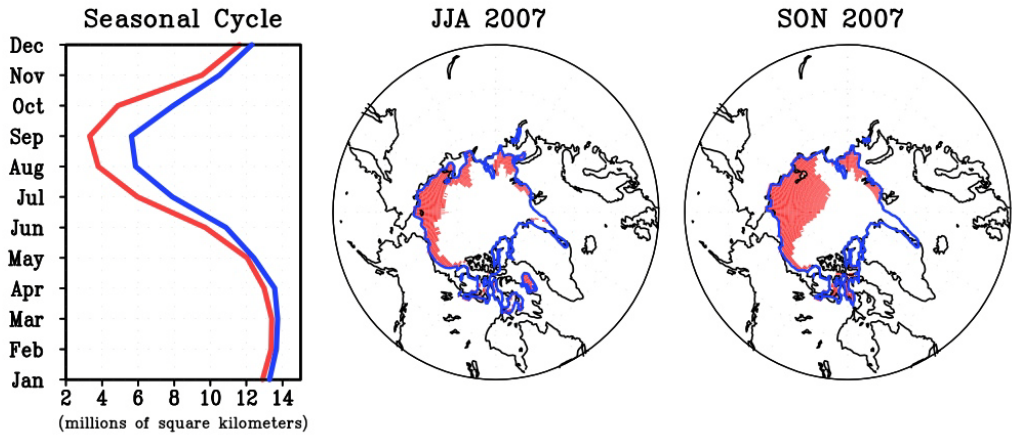
Seasonal Cycle
Dec
Nov
Oct
Sep
Aug
Jul
Jun
May
Apr
Mar
Feb
Jan
2 4 6 8 10 12 14
(millions of square kilometers)
JJA 2007
SON 2007

Figure 1

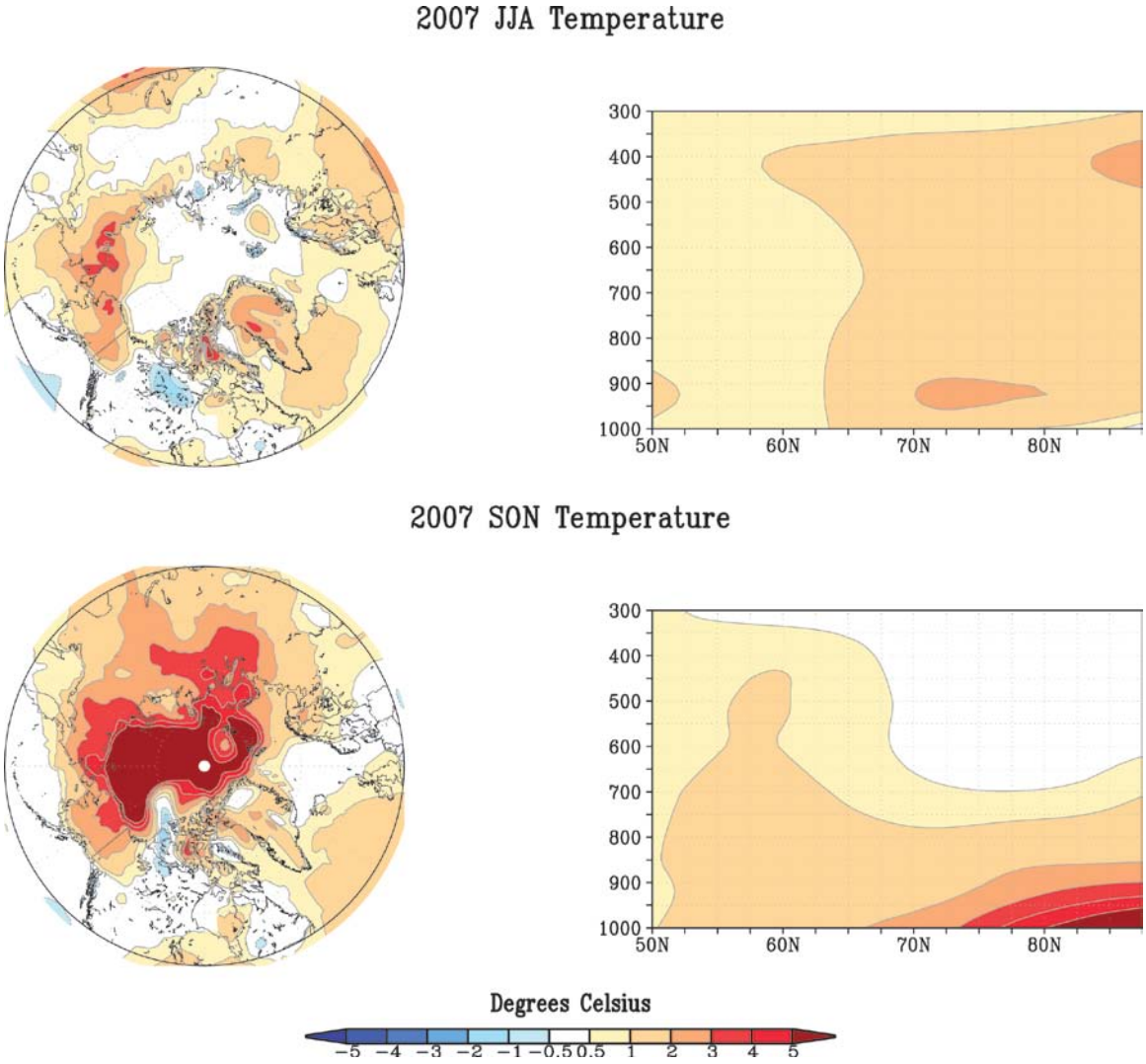
2007 JJA Temperature
300
400
500
600
700
800
900
1000
50N
60N
70N
80N
2007 SON Temperature
300
400
500
600
700
800
900
1000
50N
60N
70N
80N
Degrees Celsius
−5 −4 −3 −2 −1 −0.5 0.5 1 2 3 4 5

Figure 2

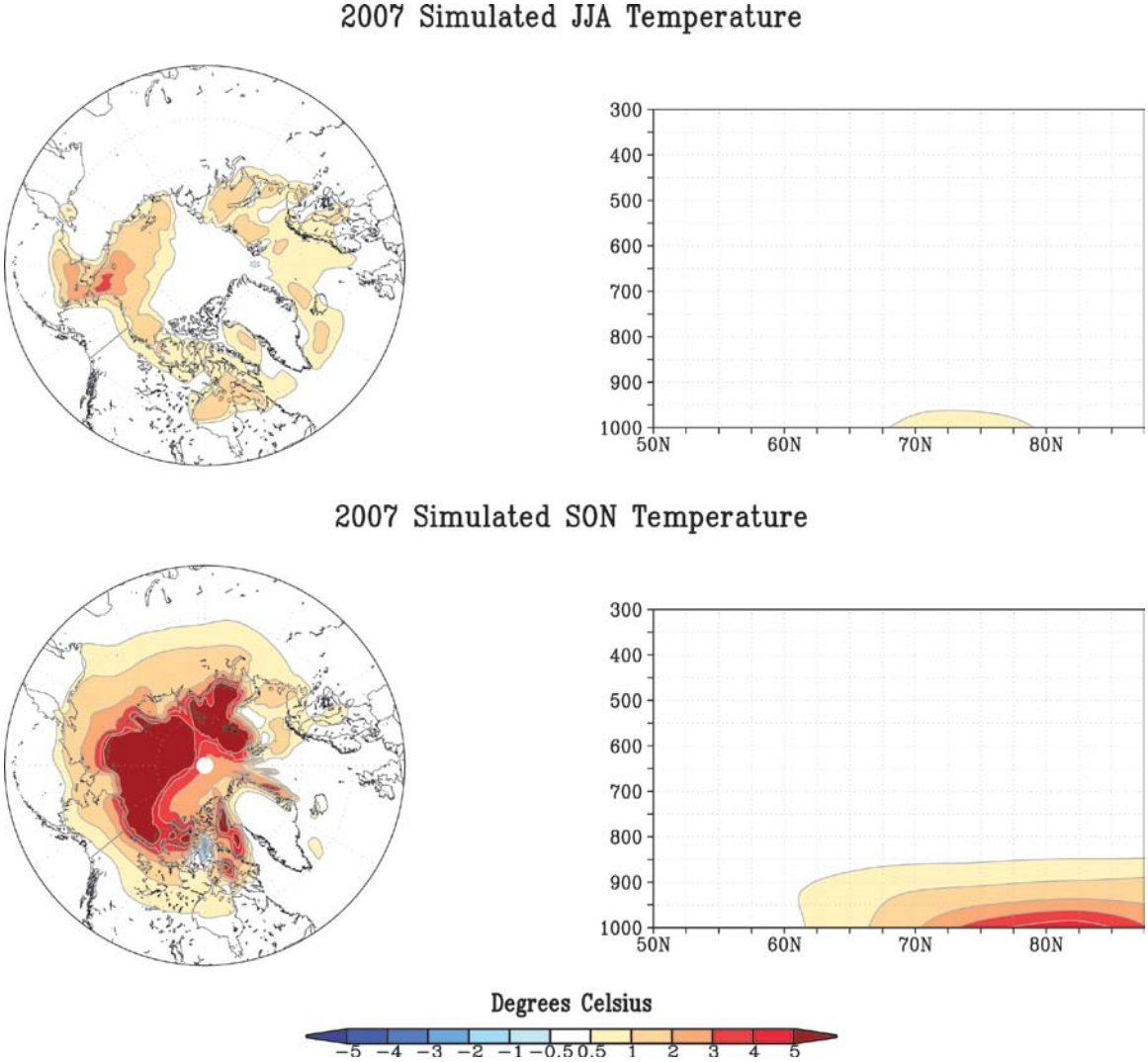
2007 Simulated JJA Temperature
300
400
500
600
700
800
900
1000
50N
60N
70N
80N
2007 Simulated SON Temperature
300
400
500
600
700
800
900
1000
50N
60N
70N
80N
Degrees Celsius
−5 −4 −3 −2 −1 −0.5 0.5 1 2 3 4 5

Figure 3

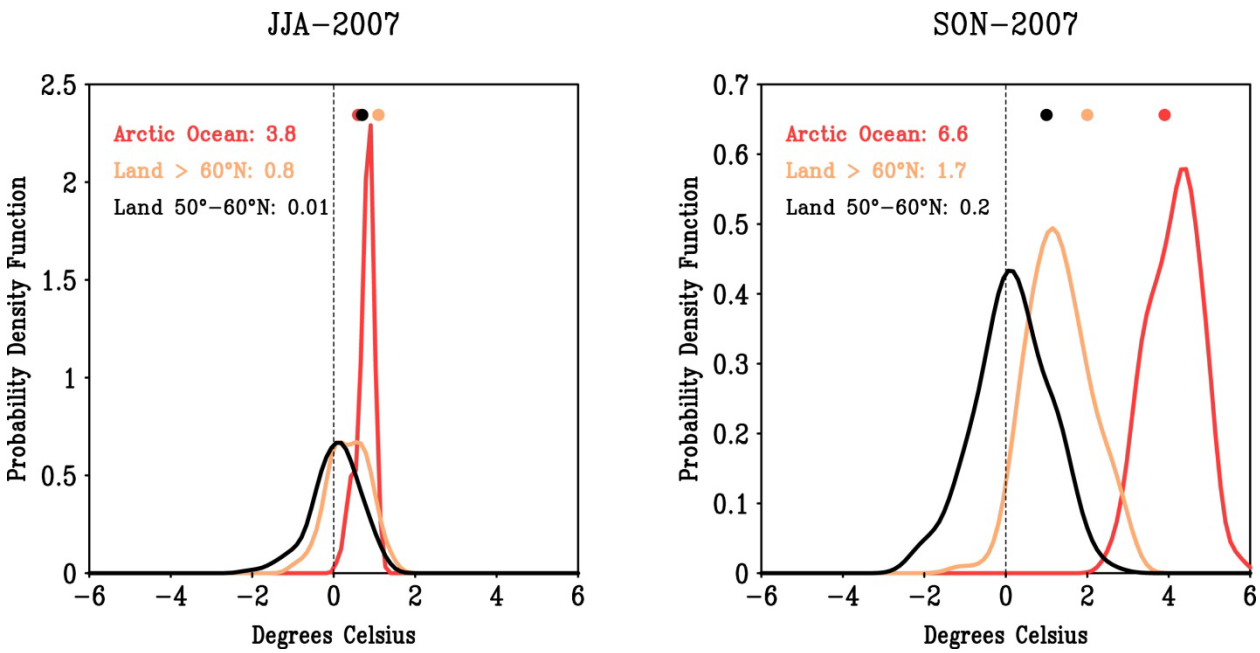
JJA−2007
SON−2007
Arctic Ocean: 3.8
Land > 60°N: 0.8
Land 50°−60°N: 0.01
Arctic Ocean: 6.6
Land > 60°N: 1.7
Land 50°−60°N: 0.2
Probability Density Function
Degrees Celsius

Figure 4